Electromagnetic pulse crimping of axial form fit joints *

K. Faes[1], O. Zaitov[1], W. De Waele[2]

[1] Belgian Welding Institute, Ghent, Belgium.
[2] Laboratory Soete, Ghent University, Ghent, Belgium

Abstract

Electromagnetic pulse crimping of form fit joints was investigated using tubes in the aluminium alloy EN AW-6060, with a diameter of 50 mm and a wall thickness of 1,5 mm. First the influence of the charging voltage and the geometrical groove parameters on the deformation behaviour and localised thickness reduction of the tube wall was investigated. The experimental results provided data for optimising the groove design.

The Design of Experiments method was used to optimise the shape and dimensions of the internal workpieces with a double groove design. Results of tensile tests on the crimp joints allowed determining the most important parameters for the groove design. Based on these observations an optimal double groove joint design was proposed.

The deformation and failure behaviour of the crimp joints during tensile testing were experimentally studied using the digital image correlation technique. This technique was used to measure the local and global deformation of the joint. Failure mechanisms include pull-out, local shearing and fracture of the tube. Three main failure modes were observed.

Keywords

Electromagnetic joining, Axial crimp joints, Design of Experiments

---

* *This work is based on the results of the CorNet collective research project "PULSCRIMP"; the authors would like to thank IWT (Agency for Innovation by Science and Technology) for its financial support.*

1 Electromagnetic Pulse Joining

The electromagnetic pulse technology uses magnetic forces to deform and/or join work-pieces. The energy stored in a capacitor bank is discharged rapidly through a magnetic coil. Typically a ring-shaped coil is placed over a tubular workpiece. When deforming tubular products, the magnetic field produced by the coil generates eddy currents in the tube. These currents, in turn, produce their own magnetic field. The forces generated by the two magnetic fields oppose each other. Consequently, a repelling force between the coil and the tube is created. As a consequence, the tube is collapsed onto an internal workpiece, creating a crimp joint or a welded joint. In the electromagnetic pulse crimping process, no atomic bond is obtained; these joints obtain their strength from the combination of an interference and a form fit. A special profiled internal workpiece is therefore used.

2 Literature Survey

In [1] the influence of the groove shape of form fit joints was investigated. Three different shapes were taken into account; triangular, circular and rectangular grooves (see Figure 1). Joints with triangular grooves were always the weakest. The explanation was that in this case the angle α is larger than for rectangular or circular grooves. This results in a lower degree of tube deformation at the groove edge, and thus a smaller tensile force is required to initiate pull-out of the tube from the groove.

Circular grooves result in a smaller angle α than the rectangular grooves, but the latter requires a larger pull-out force, due to the larger amount of shearing of the tube at the groove edges. This provides a better interlock of the tube in the groove. Joints formed with rectangular grooves always exhibit the highest joint strength, which was experimentally verified [1].

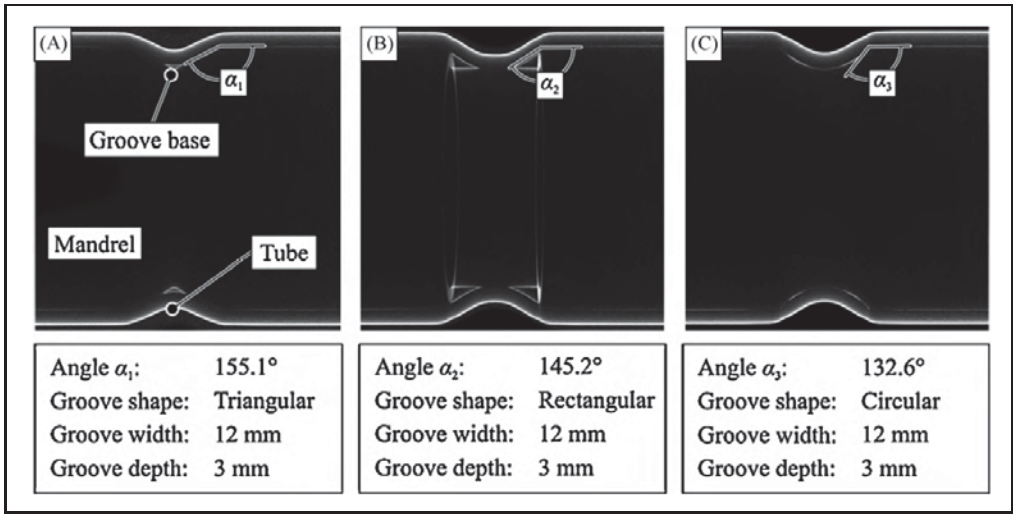

Figure 1: *Radioscopic images after deformation [1]*

The strength of form fit joints with rectangular grooves strongly depends on 3 factors determining the groove geometry: the depth, width and the groove edge radius. Deeper grooves will lead to higher joint strengths [2,3], but increasing the groove depth too much

leads to a decrease of the strength as a result of intense shearing at the groove edges during forming [4]. For the groove width, it was first believed that a narrower groove would lead to higher joint strengths [2,3], but this was later revised because an increasing groove width leads to a larger contact area at the groove base, which leads to a larger interference fit and a stronger joint strength. It can not be increased too much, because this could lead to wrinkling, which has a negative effect on the joint strength [4]. Furthermore, economical factors come into play, because a larger width requires more overlap (more material) and a higher energy. A smaller edge radius leads to a higher joint strength, but a too small radius leads to an increase of shearing at the groove edge during forming and negatively affects the joint strength [4].

In [5], the quasi-static performance of tubular joints produced with different mandrel materials were analyzed, together with the influence of process parameters. Therefore, experimental investigations on aluminium tubes (AA6060) joined on mandrels made of different aluminium, copper, and steel alloys were carried out.

Joining of profiles to lightweight frame structures by both expansion and compression has been examined in [6]. The necessary forming pressure for the joining by forming processes was applied to tubular workpieces by a medium (hydroforming) and by a magnetic field (electromagnetic compression).

In [7,8], joining by EMF was investigated as a pre-study for applying to an automotive spaceframe. Finite element simulations and strength tests were performed to analyze the influence of the geometric parameters on the joint strength. Based on these results, configurations of axial joint and torque joint were suggested and guidelines for designing the joints were established.

3 Overview of the Experiments

Electromagnetic pulse crimping of form fit joints was investigated, using tubes made of the aluminium alloy EN AW-6060 T6. The tubes had a diameter of 50 mm and a wall thickness of 1,5 mm. Solid internal workpieces were used made of the same alloy.

The experiments were performed using a Pulsar model 50/25 system with a maximum charging energy of 50 kJ (corresponding with a maximum capacitor charging voltage of 25 kV) and a discharge circuit frequency of 14 kHz. The total capacitance of the capacitor banks equals 160 µF. The pressure resulting from the magnetic flux induced by a 5-turn aluminium coil (length: 100 mm, internal diameter: 165 mm) is concentrated over the processing area using a conical field concentrator with a width of the workzone equal to 15 mm [9]. The crimp joints were produced using a single pulse.

In a first phase, the tube deformation behaviour into a groove was investigated using a special-designed cylinder system, which allowed simulating a groove with certain dimensions. The radial inward tube deformation and thickness reduction at the groove edges was measured as a function of the groove dimensions and the discharge energy.

Using this data, the shape and dimensions of the internal workpiece of crimp joints with a double groove design were optimised. The Design of Experiments method was used and a test-matrix with 64 experiments was generated. The joint tensile strength was used as the evaluating parameter.

Finally, the deformation behaviour of the crimp joints with a double groove design during tensile testing was studied using the Digital Image Correlation technique (DIC). DIC

provides results concerning displacement and strains, which can be used to have an idea about the load distribution over the 2 grooves during tensile testing.

4 Free Deformation Experiments

4.1 Introduction

During exploratory crimp joint experiments, it was observed that it is a challenge to determine the appropriate energy settings (capacity charging voltage) for a given groove design. If the voltage level is set too low, the tube will not deform into the groove and the connection will hardly have any strength. On the other hand, if too much energy is used, the tube will deform too much into the groove, and thickness reduction at the groove edges will be too severe and the internal workpiece will act as a cutting tool. Therefore it was be helpful to compose graphs which relate the radial inward tube displacement and tube wall thickness reduction at the groove edges with the applied energy level. This provides a first estimate of the charging voltage level to be applied.

In order to be able to generate these graphs with low material resources and with a low processing and evaluation time, a test setup inspired on [1] was designed and built. The system offered the flexibility to simulate a large amount of grooves, without manufacturing an internal workpiece for every test condition. The 3 parameters which were varied during these experiments are:

- the groove edge radius: set at 0,5 mm, 1,0 mm and 1,5 mm,
- the groove width: varied between 6 and 14 mm, with a 2 mm interval,
- the applied charging voltage: it was observed that 5 kV (2 kJ) was the minimum charging voltage required to deform the utilised tubes. This charging voltage was used as the lower value. The maximum voltage that could be applied without cutting the tube varied between 10 and 13 kV, depending on the combination of the previous 2 parameters.

For each of the 132 samples produced, the largest radial inward displacement and the tube wall thickness reduction at the groove edges were measured. It should be noted that the radial inward displacement was never restricted (free deformation).

Mechanical interlock behind the groove edge is the most important strengthening mechanism for a crimp joint. It is therefore important to be able to estimate tube thickness reduction at the edge of a groove. Each of the deformed tubes was cross-sectioned and the tube wall thickness was measured at four locations: the 2 upper edges and the 2 lower edges. See Figure 2 for an example of such measurements at the 2 upper edges. The average of these four values was determined in order to exclude measurement inaccuracies.

The relationship between the groove width and the radial inward displacement is directly proportional: a larger radial inward displacement is measured when the groove width is larger. This can be explained by considering the tube as a beam imposed on two supports. If these supports are close together (i.e. a small groove width), the tube is stiff and it is difficult to deform the tube into the groove. If the supports are more separated, the tube is slender and less stiff and it is easier to deform the tube into the groove. In

Figure 3 (left), the results are shown for a groove edge radius of 0,5 mm. It was also observed that the groove edge radius has a very limited influence on the radial inward tube displacement.

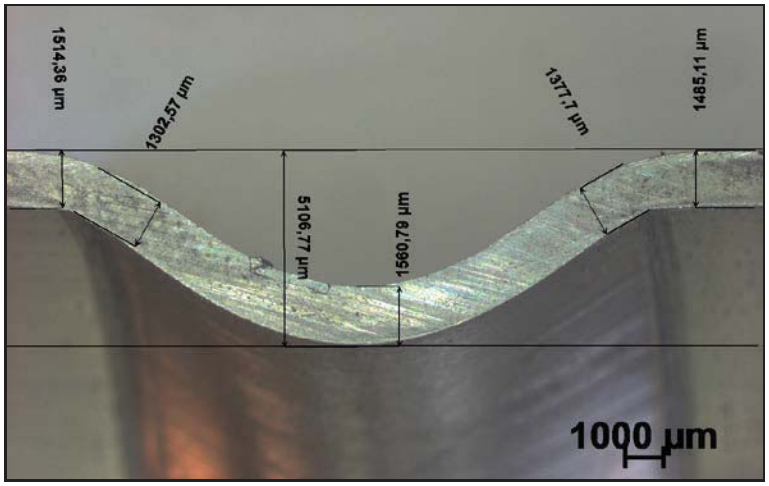

Figure 2 : *Measurement of the radial inward displacement and the wall thickness reduction at the edges of the upper half of a cross sectioned deformed tube*

More thickness reduction of the deformed tube occurs at the groove edge when the charging voltage is higher. The cause of this is the larger radial inward displacement when the voltage is higher. A remarkable trend was observed when relating the amount of thickness reduction to the groove width: first the thickness reduction increases when the groove width increases. It reaches a maximum and then the thickness reduction starts to decline again as the groove width further increases. In Figure 3 (right), the results are shown for a groove edge radius of 0,5 mm. This is an interesting observation, especially when keeping in mind that the radial inward displacement linearly increases with the groove width (see Figure 3, left). The explanation for this trend can be found in the relationship between shearing and bending deformation of the tube for different groove widths. If the groove width is small, bending of the tube into the groove is limited, and the radial inward displacement is mostly achieved by shearing at the groove edges. This causes fairly large thickness reduction for a relatively small radial inward displacement. As the groove width increases, the radial inward displacement is larger and the thickness reduction increases until a maximum is a reached. This is because the part of the displacement due to bending is still small and the larger radial inward displacement requires more shearing at the edges.

If the groove width further increases, the tube bending starts to have a significant effect. A part of the radial inward displacement into the groove is then realised by bending, which does not cause thickness reduction at the groove edges. The remaining energy after bending of the tube is then used to realise the rest of the radial inward displacement by shearing at the groove edges. As the groove width increases, a greater part of the radial inward displacement is done by bending and a smaller part by shearing at the groove edges. This explains how a larger radial inward displacement is possible in combination with a declining percentage of thickness reduction.

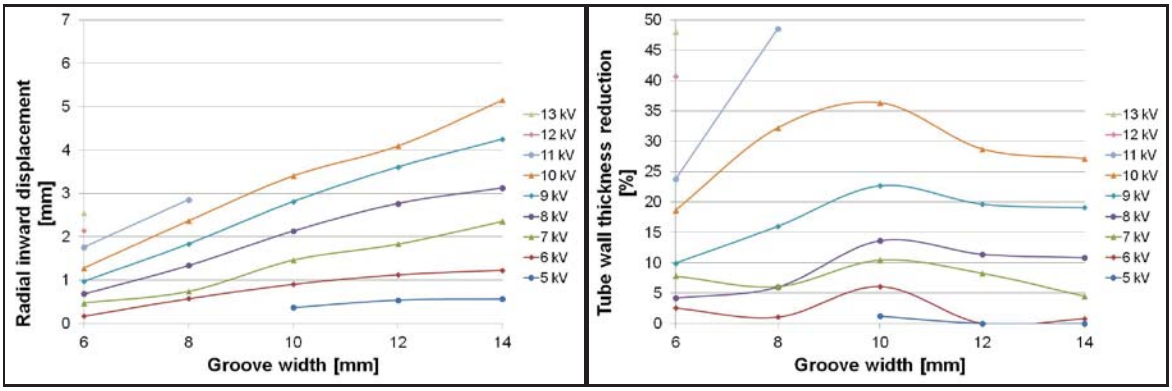

Figure 3 : *Radial inward displacement (left) and thickness reduction (right) as function of the groove width and the charging voltage for a groove edge radius of 0,5 mm*

5 Crimp Joint Parameter Optimisation Using Design of Experiments

5.1 Introduction

During preliminary experiments, it was demonstrated that an axial crimp joint with a double groove design leads to a higher tensile strength than with a single groove design. In a double groove design, there are many parameters (geometrical and process-related parameters) which affect the joint integrity. Furthermore, these parameters can possibly have a combined effect as well.

In order to determine the optimal setting for each process parameter in a structured way, a statistical approach is often used [10,11]. The choice was made to use Design of Experiments (DoE), which is a powerful technique to investigate the influence of parameters and also the mutual interaction. The concept is to gain as much information as possible with a minimal amount of experiments. In general, to investigate the influence of n parameters at two levels, 2^n experiments are required. DoE selects a subset, thus reducing the amount of experiments. This causes a certain loss of information, but it is still possible to draw statistically sound conclusions if the subset is well chosen. This reduction of experiments is of great importance because costs can be reduced and time demanding analysis can be performed only on relevant specimens.

The preliminary experiments and the free deformation experiments were required to use DoE in an effective way. The results of those experiments offered the possibility to make well-founded choices for selecting the most important parameters and for determining realistic values for these parameters.

5.2 Parameter Values

A 2-level design was used, so each parameter was varied at two values. These values must be chosen wisely and must meet two conditions. First, the difference between the two values should be maximal. Second, the values of the different parameters must be

combinable and realistic. Based on the previous experiments, the following values have been chosen (see also Figure 4 and Figure 7).

	Parameter	Lower value	Upper value
X1	Radius of edge 1_1	0,5 mm	1,5 mm
X2	Collar depth	0,0 mm	1,0 mm
X3	Charging voltage	10,5 kV	12,0 kV
X4	Depth groove 1	1,5 mm	3,0 mm
X5	Depth groove 2	2,5 mm	4,0 mm
X6	Radius of edge 2_1	0,5 mm	1,5 mm
X7	Width groove 1	6,0 mm	8,0 mm
X8	Width groove 2	4,0 mm	6,0 mm

Table 1: *Overview of the parameters' upper and lower values*

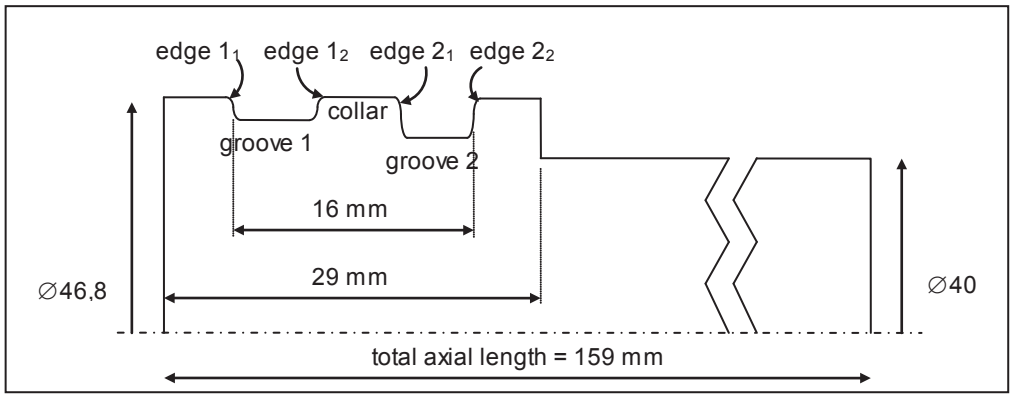

Figure 4: *Nomenclature and most important dimensions of the internal workpiece*

Performing 64 experiments allowed to investigate 22 of 28 double effects. Six double effects were confounded with each other. Each experiment was performed twice to reduce the scatter and to increase the statistical reliability (in total 128 experiments).

5.3 Results

The relative tensile strength of the crimp joints was chosen as the evaluating parameter for the DoE. This value is equal to the ratio of the tensile strength of the specimen to the tube base material tensile strength (= 225,6 MPa). Tensile testing was performed on an Instron 4505 universal testing machine. The testing machine has a load cell of 10 kN. The tensile test specimens were prepared according to the standard ASTM B221.

Table 2 lists the significant effects found by the DoE analysis. Some of them are discussed below.

Parameter	Physical interpretation	Increase of relative tensile strength [%]
X8	Second groove width	7,7
X1	Edge radius 1_1	6,3
X2	Collar depth	6,1

X4	Depth first groove	5,8
X6	Edge radius 2_1	3,7
X2*X3	Collar depth and applied voltage	3,6
X2*X8	Collar depth vs. second groove width	2,9
X3*X4	Applied voltage and first groove depth	2,7
X3*X5*X7	-	2,5
X3	Applied voltage	2,3
X1*X3*X7	-	2,1
X2*X7	Collar depth and first groove width	2,1
X4*X8	First groove depth and second groove width	1,9
X1*X2*X3	-	1,9
X3*X6*X7	-	1,9
X4*X7	First groove depth vs. first groove width	1,7
X4*X6	First groove depth vs. edge radius 2_1	1,6

Table 2: *Significant effects of the parameters*

Second groove width (parameter X8)

A width of the second groove equal to 6 mm instead of 4 mm resulted in a higher joint tensile strength. A large groove width is needed to create a better 'filling' of the groove. The width of the second groove should always be chosen large enough to allow a sufficient deformation of the tube into the groove. When the distance between the two supports increases, the tube can more easily be deformed between the supports. The angle θ in Figure 5 provides an indication for the mechanical interlock. The smaller the angle θ, the more mechanical interlock is possible. Also, as was concluded during the free deformation experiments, a short groove will cause more shearing which results in more tube wall thickness reduction than with a long groove.

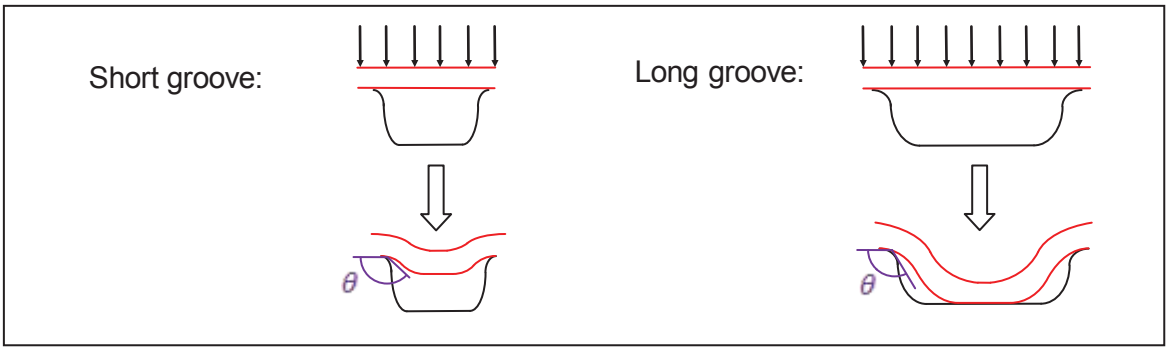

Figure 5: *Influence of the groove width on the mechanical interlock*

Edge radius 1_1 (parameter X1)

In contrast to what initially was thought, a small edge radius is desired for edge 1_1. The first edge bears the major part of the axial load and thus there is a need for a good mechanical interlock. A sharp edge cannot be defined in values, but it can be stated that for this design, it is better to use an edge radius of 0,5 mm than an edge radius of 1,5 mm.

Collar depth (parameter X2)

For the optimal design, the collar depth must be chosen equal to 1 mm. During the tensile tests, it was demonstrated that all designs with a sunken collar had a higher tensile strength than those without. This can be attributed to the fact that with a sunken collar, the tube first deforms into the gap covering the two grooves and later, when making contact with the collar, starts deforming in each groove separately (see Figure 6). When the tube deforms into a large gap, it acts like a beam imposed onto two supports with a large distance between the supports, under a vertical evenly distributed load (the magnetic repulsive force from the coil). In Figure 6.A, the tube is divided into two beams imposed onto two supports, each with a small gap length. The tube experiences more shearing stress and less bending moment than in Figure 6.B. For an equal applied voltage and similar groove geometries in A and B, thickness reduction in edge 1_1 and edge 2_2 will be less excessive in case B.

It should be noted that in case A, the area of largest radial displacement of the deformed tube is approximately in the middle of each groove, while in case B this area of the tube is found closer to the central collar. The dotted vertical lines below the right part of Figure 6 indicate the position of these zones of maximal radial displacement. When these lines are positioned closer to the collar, a stronger mechanical interlock is obtained in the second groove. On the other hand, less mechanical interlock is obtained in the first groove, but this negative effect is compensated with less thickness reduction at edge 1_1.

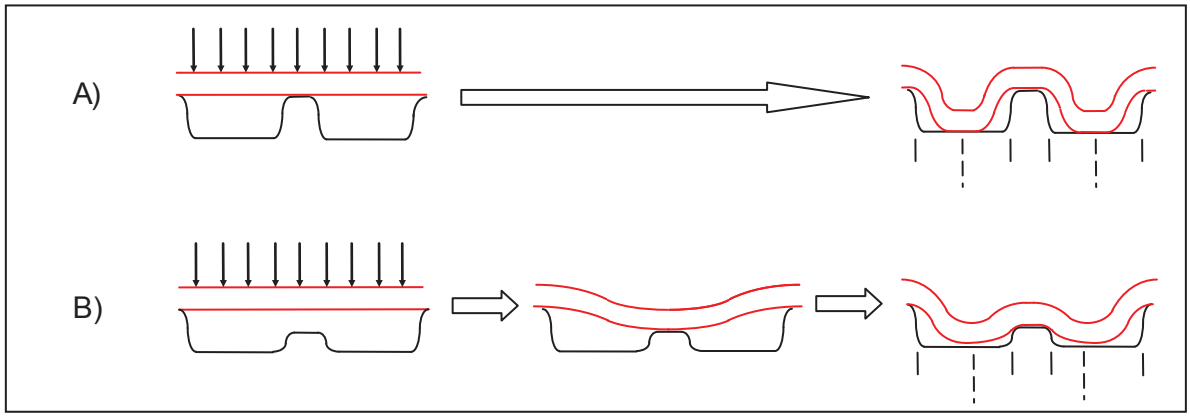

Figure 6: *A sunken collar leads to less thickness reduction and better interlock at the second groove.*

Depth of the first groove (parameter X4)

It was found that it is beneficial to have a small depth of the first groove. This can be explained by the fact that the thickness reduction at edge 1_1 will be less and so a sharper edge radius 1_1 can be allowed. This is beneficial because it creates a stronger mechanical interlock.

Edge radius 2_1 (parameter X6)

Again, a sharp edge 2_1 is desirable to create mechanical interlock in the second groove.

Collar depth and applied voltage (parameters X2*X3)
This second order effect contains the collar depth (parameter X2) and the applied voltage (parameter X3). As can be seen in Figure 6, when using a sunk collar, a high voltage is required to first bend the tube into the large gap covering the two grooves and to subsequently sufficiently deform the tube in each groove separately, while consuming some of the energy for the deformation of the central collar.

Collar depth and second groove width (parameters X2*X8)
As already described above, with a sunken collar the zone of maximal radial displacement is closer to the collar. This induces an increase of mechanical interlock at the second groove. Furthermore, when a larger second groove is present, the tube more easily deforms into the second groove, increasing the mechanical interlock even more. The increase of mechanical interlock due to a larger second groove in combination with a sunken collar also involves minimisation of the tube wall thickness reduction at the edges.

Charging voltage and first groove depth (parameters X3*X4)
A shallow first groove in combination with a large charging voltage is preferred over a deep first groove in combination with the same large charging voltage, because there will be more contact and thus more interference fit when the groove is shallow.

Charging voltage (parameter X3)
It is clear that a larger charging voltage causes more deformation and more filling of the tubes into the grooves, which results in more mechanical interlock and possibly some interference fit on the bottom of the grooves as well.

The following second order effects are less significant and are not discussed in detail:

- Collar depth and first groove width (parameters X2*X7)
- Depth of first groove and width of second groove (parameters X4*X8)
- Depth of first groove and width of first groove (parameters X4*X7)
- Depth of first groove and edge 21 (parameters X4*X6)

5.4 Conclusion

To propose a suitable design for a double grooved axial crimp joint providing a sufficient tensile strength, the following points of attention should be kept in mind: the critical zone where most crimp joints fail is located at edge 1_1. Therefore, tube wall thickness reduction should be minimised in this location, but keeping in mind that some thickness reduction is inevitable.

A wide shallow first groove with a sharp edge 1_1 is beneficial to obtain a higher tensile strength. The sharp edge is required to create interlock, while the groove width and shallow depth create a good filling and minimise tube thickness reduction.
It is important to have a central collar which is sunk below the specimen surface to further minimise the tube thickness reduction at edge 1_1 and 2_2 and to better distribute the tensile strength over the two grooves. With a sunken central collar, the mechanical interlock in the second groove is increased. It is also preferred that the second groove is wide, with a

sharp edge 2_1. The second groove width should be long enough so the tube can easily deform into the groove and realise a good filling.

In Figure 7, the parameters of the optimal design of the internal workpiece are indicated in bold. With these parameters, the tensile strength of the crimp joint was equal to the tensile strength of the tube base material.

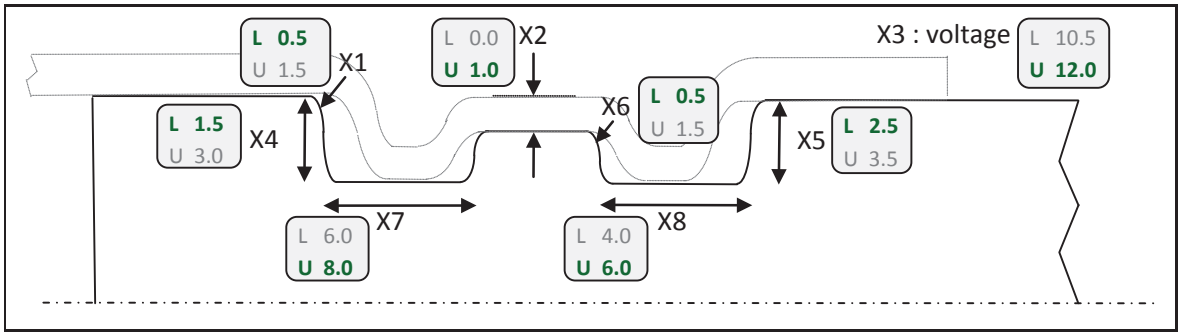

Figure 7: *Parameters (in mm) used in the DoE test matrix (in mm and kV), with the lower (L) and the upper (U) values. The optimal values are marked in bold.*

6 Failure Modes

6.1 Introduction

The Digital Image Correlation (DIC) technique was used to investigate the failure behaviour of the axial joints with a double groove design subjected to an axial load. The DIC method allows deducing the material displacement during tensile testing by tracking the deformation of a random speckle pattern by acquired digital images. The image analysis process can be understood as a pattern recognition technique, which searches locally the random speckle pattern by comparing the images of the deformed with the reference state. By using two synchronised cameras which acquire images of the loaded specimen from different viewing angles, it is possible to determine both the three-dimensional displacement and deformation as a function of time [12].

Figure 8: *Detail of the test specimen with white layer and black speckle pattern*

After tensile tests were performed on the first series of 64 experiments of the DoE, the relative tensile strength versus displacement curves were analysed and 32 interesting crimp joints were selected to be analysed with the DIC technique during the second series

of tensile tests. It was found that the failure behaviour of the crimp joints can be divided into 3 main failure modes:

- Failure mode 1: the tube tears at edge 1_1 at the complete circumference.
- Failure mode 2: the tube tears at edge 2_1 at the complete circumference.
- Failure mode 3: the tube is pulled of the internal workpiece, and no tearing occurs.

In **failure mode 1**, the tube wall thickness reduction near groove edge 1_1 and the amount of load taken up by the second groove determines the joint tensile strength. After the tube breaks at edge 1_1, the joint can no longer bear a load.

It was also observed that failure mode 1 can be divided into 3 subgroups:

- Subgroup 1: These crimp joints have an inappropriate design of the first groove. As a consequence, the tube wall thickness reduction at edge 1_1 is too excessive and the second groove doesn't bear any part of the load. Based on the tensile tests performed during the DoE-experiments, it was found that in this case the average relative tensile strength was equal to 74%.
- Subgroup 2: These crimp joints have a better design of the first groove, allowing also the second groove to bear part of the load. The internal parts however didn't have a sunken collar. The average relative tensile strength was equal to 80%.
- Subgroup 3: These crimp joints have an even better design of the first groove, as well as a sunken collar with a depth of 1 mm, which causes less thickness reduction at groove edge 1_1 and which allows the second groove to bear a larger part of the load. The average relative tensile strength was in this case 91%.

In **failure mode 2**, the tube wall thickness reduction near groove edge 2_1 determines the tensile strength, until the tube breaks at this edge. This corresponds with point A in Figure 9, and with Figure 11 (graphically showing the Z-displacement for a crimp joint failed by failure mode 2). It was observed that the connection still has some strength after this fracture (point B). This is because at this moment the load-bearing mechanism changes: the tube now needs to be pulled out of the first groove without thickness reduction, and thus is the load-bearing capacity is determined by the tube interlock in the first groove in combination with the relative axial displacement between the tube and the internal workpiece at the edge 1_1. The curve of the relative tensile strength versus displacement increases then to a second (lower) maximum (see point C in Figure 9 and Figure 12). Point C corresponds with maximal interlocking. Thereafter, the load decreases to zero, since the tube experiences little resistance when the displacement further increases. The tube which was originally deformed into the first groove is almost completely pushed back to its original position before the crimping operation. The average relative tensile strength of the joints which failed by failure mode 2 was equal to 75,3%.

In **failure mode 3** no tearing occurs, and thus it is the radial inward tube displacement into both grooves in combination with the axial displacement of the tube relative to the internal workpiece which is of importance. The average relative tensile strength of these joints was 66,4%.

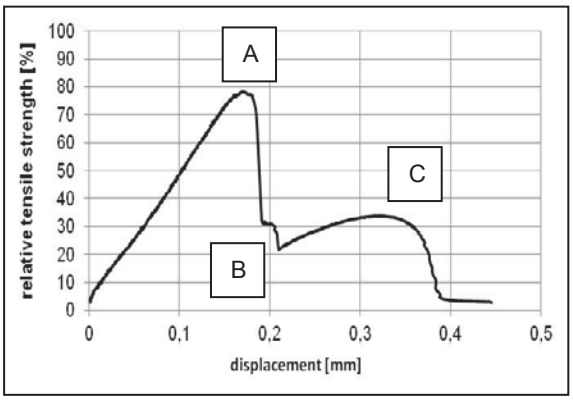

Figure 9: *Relative tensile strength versus displacement curve of a joint failed by failure mode 2*

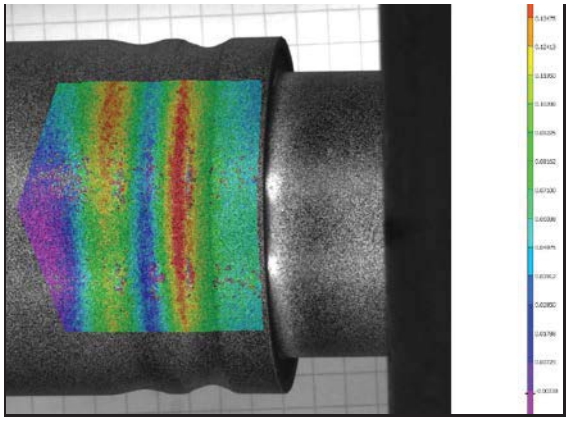

Figure 10: *The tube gets pulled out of groove 1 and 2*

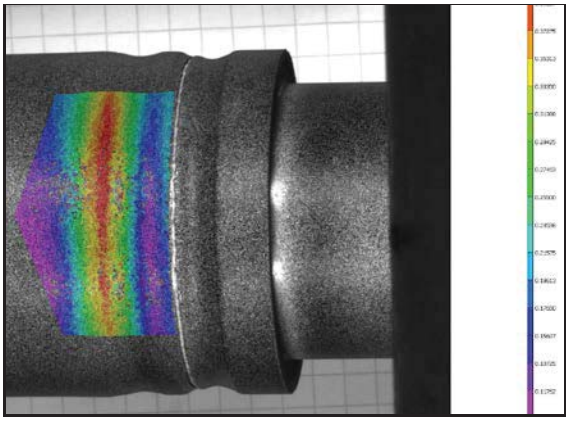

Figure 11: *The tube tears at edge 2_1*

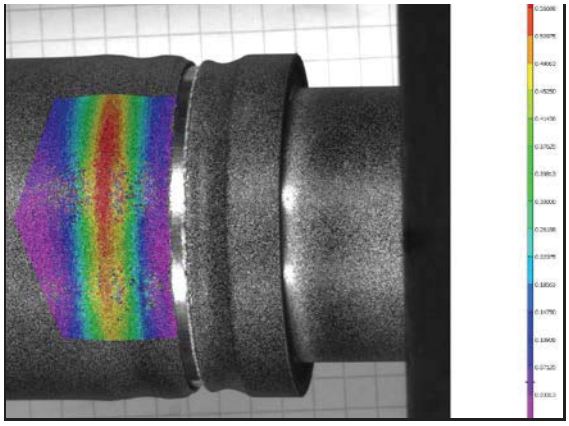

Figure 12: *The tube is pulled out of the first groove (without thickness reduction or fracture)*

7 Conclusion

Electromagnetic pulse crimping of form fit joints was investigated using tubes in the aluminium alloy EN AW-6060. The tube deformation behaviour for a single groove design was investigated using a cylinder system which allowed to simulate a groove with certain dimensions. It was concluded that the relationship between the groove width and the radial inward displacement is directly proportional and that a higher capacitor charging voltage leads to a larger radial inward displacement. A remarkable trend was observed when relating the tube wall thickness reduction to the groove width: initially thickness reduction increases, but as the groove width increases, thickness reduction declines again. This was explained by looking at the ratio of shearing and bending.

The Design of Experiments method was used to optimise the shape and dimensions of the internal workpieces with a double groove design. A test-matrix with 64 experiments was generated. The tensile strength of the crimp joints was chosen as the evaluation parameter. An optimal design was proposed, which had a statistically expected tensile strength equal to the tensile strength of the tube base material. The optimal design

includes a shallow, long first groove with sharp edges, a sunken central collar and a long and deeper second groove with sharp edges.

The deformation behaviour of the crimp joints with a double groove design during tensile testing was studied using the Digital Image Correlation technique. Three main failure modes were observed. The failure mode in which the tube tears at the first edge of the first groove occurred most during the performed experiments and resulted in the highest tensile strength.

References

[1] Weddeling, C., Woodward, S., Marré, M., Nellesen, J., Psyk, V., Tekkaya, E., Tillmann, W.: Influence of groove characteristics on strength of form-fit joints. Journal of Materials Processing Technology, Vol. 211, Issue 5, 2011, p. 925 -935.

[2] Bühler, H., von Finckenstein, E., Fügen durch Magnetumformung. Werkstatt und Betrieb 101, 1968: p. 671-675.

[3] Golavashchenko, S. Methodology of design of pulsed electromagnetic joining of tubes. Proceedings of the TMS Symposium "Innovations in Processing and Manufacturing of Sheet Materials". 2001. New Orleans, LA, USA.

[4] Park, Y., Kim, H., Oh, S., Design of axial/torque joints made by electromagnetic forming. Thin walled structures 43, 2005: p. 826-844.

[5] Barreiro, P., Schulze, V., Löhe, D., Marre, M., Beerwald, C., Homberg, W., Kleiner, M.: Strength of Tubular Joints Made by Electromagnetic Compression at Quasi-static and Cyclic Loading. High Speed Forming 2006, Proceedings of the 2nd International Conference, Dortmund, 20.-21.03.2006, p. 107-116.

[6] Marré, M., Brosius, A, Tekkaya, A.E. Joining by Compression and Expansion of (None-) Reinforced Profiles. Advanced Materials Research Vol. 43, 2008, p. 57-68

[7] Park, Y.-B., Kim, H.-Y., Oh, S.-I. Design and Strength Evaluation of Structural Joint Made by Electro-Magnetic Forming (EMF). Proceedings of the 8th International Conference on Numerical Methods in Industrial Forming Processes. AIP Conference Proceedings, Vol. 712, p. 1476-1484 (2004).

[8] Park, Y.-B., Kim, H.-Y., Oh, S.-I. Joining of thin-walled aluminum tube by electromagnetic forming (EMF). International Journal of Automotive Technology, Vol. 6, No. 5, p. 519-527 (2005).

[9] Faes, K.; Baaten, T.; De Waele, W.; Debroux, N.: Joining of Copper to Brass Using Magnetic Pulse Welding. Proceedings of the International Conference of High Speed Forming, Columbus, Ohio, 9 - 10 March 2010.

[10] Altekar, M., et al.: Assay Optimization: A Statistical Design of Experiments Approach. Journal of the Association for Laboratory Automation, 2006. 11(1): p. 33-41.

[11] Bahloul, R., et al., Sheet metal bending optimisation using response surface method, numerical simulation and design of experiments. International Journal of Mechanical Sciences, 2006. 48(9): p. 991-1003.

[12] Sutton, M.A., Orteu, J., Schreier, H.W., Image correlation for shape, motion and deformation measurements, Springer Science, 2009. ISBN 978-0-387-78746-6.